Appl. Phys. B 78, 443–446 (2004)
DOI: 10.1007/s00340-003-1391-4

Applied Physics B
Lasers and Optics

D. DIESING[1]
M. MERSCHDORF[2]
A. THON[2]
W. PFEIFFER[2,✉]

Identification of multiphoton induced photocurrents in metal–insulator–metal junctions

[1] Institut für Schichten und Grenzflächen, Forschungszentrum Jülich, 52425 Jülich, Germany
[2] Physikalisches Institut, Universität Würzburg, 97074 Würzburg, Germany

Received: 16 September 2003 /
Revised version: 21 November 2003
Published online: 3 February 2004 •

ABSTRACT Illumination of metal–insulator–metal junctions with ultrashort laser pulses and multiphoton electron excitation in the top electrode leads to the injection of electrons into the backside electrode. Time resolved photocurrent spectroscopy shows that the carrier injection is not instantaneous but occurs with an effective lifetime of about 30 fs. The observation of an effective lifetime reveals that photon-assisted tunneling is negligible. It is shown that three-photon induced internal photoemission and two-photon induced tunneling of excited electrons are the dominating transport mechanisms.

PACS 73.40.-c; 72.10.-d; 73.40.Gk; 73.50.Pz

Tunnel processes are strongly influenced by an oscillatory perturbation of the tunnel barrier, e.g., an interaction with light or an applied ac bias. The increase of the tunnel current due to photon-assisted tunneling (PAT) was first demonstrated in superconducting metal–insulator–metal junctions (MIM) under microwave irradiation [1]. The theory for this experiment by P.K. Tien and J.P. Gordon [2] is still widely used to explain photon-assisted tunneling phenomena in the perturbation limit (see e.g. transversal times for tunneling [3]). However, recent theoretical work demonstrates that photon-assisted tunneling beyond the perturbation limit gives rise to fascinating phenomena like coherent destruction of tunneling [4], coherent control of electron currents in double barrier structures [5, 6] and rectification currents in molecular wires [7]. Experiments using semiconductor devices under 60 GHz irradiation show that photon-assisted tunneling allows the electrical currents to be controlled [8]. It is important to note that the phase coherence of the involved quantum mechanical states is essential for photon-assisted tunneling to occur. As a consequence, the experimental observation of photon-assisted tunneling has up to now been restricted to tunnel junctions and excitation conditions in which decoherence plays a minor role, i.e., the coupling of an electronic state to other excitations is smaller than the electronic coupling via the tunnel gap. Such conditions can be met in metal–insulator–metal junctions for small photon energy, i.e., microwave to mid-infrared range. In contrast, continuous wave excitation in the visible leads to the tunneling of excited electrons (sometimes denoted photon-induced tunneling [9]). In continuous wave excitation, the damage threshold of the device limits the maximum field strength. However, the use of ultrashort laser pulses could overcome this limitation. With state of the art laser technology, a maximum oscillating field strength in the range of 10^9 V m^{-1} is accessible for laser pulses of 1 nJ pulse energy [10] leading to interesting new phenomena of electron dynamics at interfaces [11]. For a typical tunnel barrier width of 1 nm, this corresponds to potential oscillations in the range of volts. Accordingly, the laser field represents a strong perturbation of the tunnel barrier. Under such conditions, photon-assisted tunneling in a MIM junction might win over the tunneling of excited electrons allowing for the above-mentioned coherent control of photon-induced currents. In the experiments presented here, the laser field induced potential oscillations in the tunnel junction is in the range of 0.1 V and one can, therefore, expect that all mentioned mechanisms contribute to the total photocurrent. However, as discussed below, both photon-assisted tunneling and tunneling of multiphoton excited electrons exhibit a nonlinear response. Therefore, it is crucial to identify the photon-induced transport mechanism. Here we present photocurrent spectroscopy experiments based on the interferometric two-pulse correlation measurements that allow the identification of nonlinear photocurrent contributions in metal–insulator–metal junctions.

In tunnel junctions under intense irradiation, different photon-induced mechanisms give rise to photocurrents. Figure 1 depicts three different contributions to the photocurrent in MIM junctions: *i*) internal photoemission, *ii)* tunneling of excited electrons, and *iii)* photon-assisted tunneling. Internal photoemission requires the excitation of electrons into states above the tunnel barrier. These electrons then cross the barrier with a probability close to unity depending on the transmission coefficients at the two interfaces. The lifetime of the excited electrons in these states, typically in the range of a few femtoseconds, and their excitation cross-section determine the magnitude of this contribution. Similar to internal photoemission, excited electrons in states well above the Fermi energy but still below the top of the tunnel barrier can contribute substantially to the tunnel current, since the effective barrier height is reduced for these electrons. Both mechanisms – in-

✉ Fax: +49-931/888-4906, E-mail: pfeiffer@physik.uni-wuerzburg.de

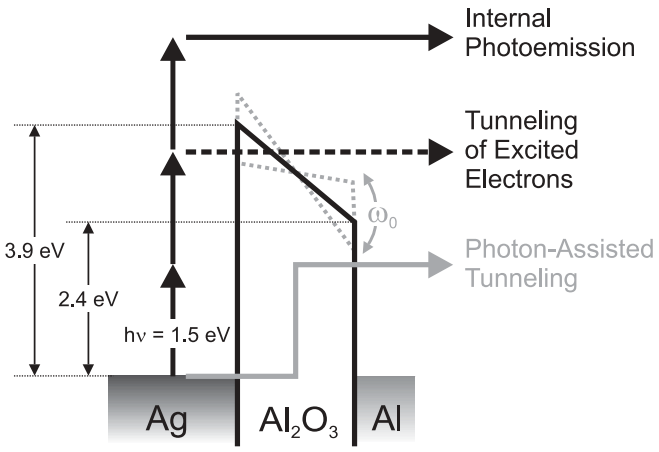

FIGURE 1 Different photocurrent contributions in a Ag–Al_2O_3–Al MIM junction under zero bias. The sequence of *vertical arrows* indicates the multiphoton excitation of electrons from the Fermi level

ternal photoemission and tunneling of excited electrons – are well described assuming a static barrier. This assumption is no longer valid for the third contribution, i.e., photon-assisted tunneling.

Under illumination, the tunnel barrier oscillates with the fundamental frequency of the applied radiation leading to a degeneracy of electronic states that are separated by multiples of the photon energy. This provides additional channels for tunneling and, therefore, influences the tunnel current. In the limit of small frequencies, i.e., a photon energy in the far to mid infrared, this photon-assisted tunneling dominates the photon-induced current and it was shown that this mechanism is equivalent to the rectification behavior of the nonlinear current–voltage characteristic of tunnel junctions [12]. Qualitatively, this could be understood as follows: The tunnel probability for an electron excited by such low-energy photons is almost the same as for an electron in the initial state. Hence tunneling of excited electrons is irrelevant, whereas the perturbation of the tunnel barrier still leads to coupling of electronic states. For excitation in the visible, however, the tunnel probability increases substantially and consequently tunneling of excited electrons becomes more important.

In general, a photocurrent through a tunnel junction can be a mixture of all three different contributions. Their relative strength then depends on the actual excitation conditions and interface properties. The argument given above shows that in the limit of high frequencies and low field strength photon-assisted tunneling can be neglected. Under these conditions, the variation of the photocurrent with photon energy directly reflects the variation of the effective tunnel matrix element [9]. However, under excitation with ultrashort laser pulses, the perturbation of the tunnel barrier can become substantial and it is not clear which mechanism is then the dominating one. In the following, we demonstrate how multiphoton photocurrent spectroscopy and two-pulse correlation measurements can be used to identify different transport mechanisms in metal–insulator–metal junctions.

Here we use Ag–Al_2O_3–Al metal–insulator–metal junctions grown on a polycrystalline ZnSe substrate as described in [13]. Tunneling spectroscopy reveals the band offsets of 3.9 eV and 2.4 eV for the Ag-oxide and the Al-oxide interface, respectively (Fig. 1). For photocurrent measurements, the sample is mounted in a liquid nitrogen cooled cryostat and is illuminated with a mode locked Ti:sapphire laser (80 MHz repetition rate, 0.1 nJ pulse energy, 1.5 eV photon energy, 20 fs pulse duration, 10 μm focus diameter, 45° incidence angle, *p*-polarization). The photon-induced current is detected using a low noise current–voltage converter (10^9 V A^{-1}) and phase sensitive detection using a lock-in amplifier. For interferometric two-pulse correlation measurements, a Mach–Zehnder interferometer generates two laser pulses with variable delay using a piezo-driven and feedback controlled delay stage. Simultaneously to the photocurrent measurements, a photodiode sensitive at 800 nm records the first order autocorrelation of the laser pulse. In addition, two-photon absorption in a wide band gap photodiode (Hamamatsu G1116) yields the second order autocorrelation. The time dependent field for a single pulse is then obtained by simultaneously fitting the first and second order autocorrelation of the laser pulses assuming a Gaussian shaped spectrum and allowing for up to fourth order phase dispersion. This field is also acting on the MIM junction since material induced dispersion is balanced in both optical pathways. To suppress the low frequency laser noise (< 20 mHz), the signal is averaged over multiple scans of the interferometer. The long-term drift of the optical path difference in the interferometer is compensated after data acquisition using the first order autocorrelation signal as a reference for the relative phase of the successive scans resulting in a standard deviation of the optical path difference of less than 30 nm.

Illumination of the MIM junction with ultrashort laser pulses generates a photocurrent through the device as shown in Fig. 2. For this measurement, the illumination is chopped and the current transients are directly recorded using a digital sampling oscilloscope. Without illumination, the current drops to zero, since no dc bias is applied to the MIM junction. After switching on the illumination, the current increases and saturates after about 30 ms at 45 pA. The capacitance of the MIM junction (≈ 500 nF) and the input impedance of the sampling oscilloscope determine the time constant for current saturation. The positive sign of the current shows that the net flow of electrons is directed from the Ag to the Al electrode. The asymmetry between the electron flow directed from Ag to Al and the opposite direction agrees well with the depth distribution of the absorbed photons since 80% of the ab-

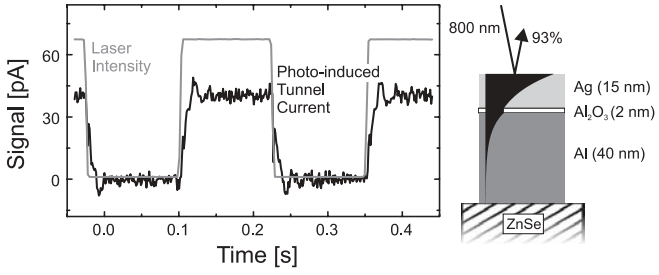

FIGURE 2 Transient of the average photocurrent with periodically modulated illumination of the MIM junction using ultrashort laser pulses (1.5 eV photon energy, 1 nJ pulse energy, 80 MHz repetition rate, 20 fs duration). The peak laser intensity is 10^{10} W cm^{-2} at the Ag surface. A cross section of the junction together with the depth distribution of the absorbed energy is shown on the *right side*

sorbed radiation is deposited in the Ag film. Accordingly, the illumination of the MIM junction with ultrashort laser pulses leads to a carrier injection into the backside electrode. From the injection current magnitude and the average incident laser power a quantum efficiency for carrier injection of about 10^{-7} per absorbed photon is estimated. For unfocused illumination (1 mm spot diameter) of the MIM junction, i.e., a four orders of magnitude lower laser intensity, the quantum efficiency for injection drops to 10^{-12}, indicating that the carrier injection mechanism must be based on a multiphoton process.

Two-pulse correlation photocurrent measurements with interferometric resolution (Fig. 3) allow the dominant transport mechanisms to be identified. At zero delay the two pulses interfere constructively and the signal is about thirty times larger than without overlap of the pulses. This enhancement and the Fourier transform of the two-pulse correlation (TPC) signal S (inset in Fig. 3a) that exhibits a spectral contribution also at the third harmonic of the fundamental frequency ω_0, but none at higher harmonics, reveal a three-photon induced current contribution. A pure three-photon process is characterized by a ratio of the TPC signal S of $S(\tau = 0)/S(\tau = \infty) = 32$, whereas a two-photon process is characterized by a ratio of 8 (e.g. see [14]). The observed signal does not quite reach this ratio. The slightly lower value stems from the finite time difference between consecutive data points and the small but not vanishing phase jitter in the Mach–Zehnder interferometer. Correcting for these effects shows that the TPC signal shown in Fig. 3a is dominated by a three-photon induced current.

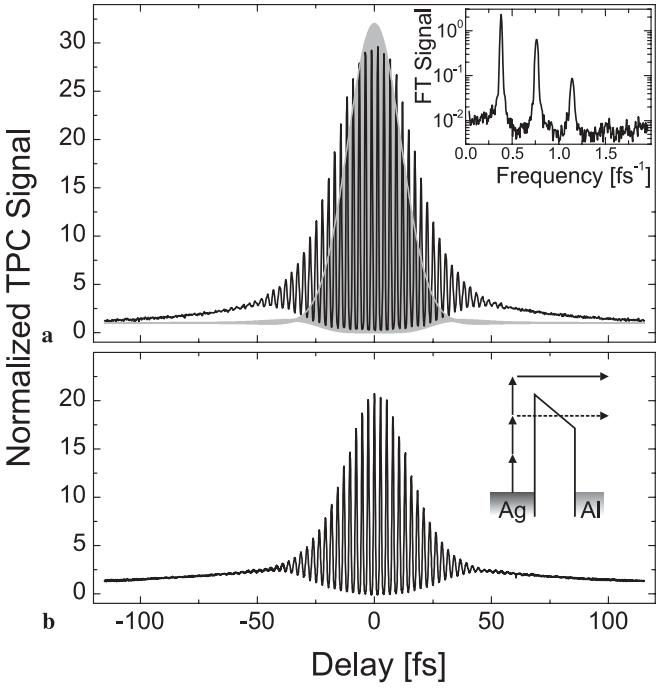

FIGURE 3 Two-pulse correlation (TPC) photocurrent signal for two metal–insulator–metal junctions, both normalized to the signal at a delay of 180 fs. The *inset* in part **a** shows the Fourier transform of the TPC photocurrent signal. The envelope of the TPC signal for a three-photon excitation assuming instantaneous response is shown in **a** as *shaded area*. **b** shows the TPC signal in another metal–insulator–metal junction that was prepared in the same way

In addition to the information about the order of the multiphoton process, the TPC signal contains also information concerning the dynamics of the process. The envelop of the calculated TPC signal assuming an instantaneous third order nonlinear process and using the actual pulse shape is shown in Fig. 3a as shaded area. The calculated TPC signal converges to one for a delay of about 50 fs indicating the delay for which the two pulses do no longer overlap. In contrast, the measured signal approaches one only for a much larger delay. This shows that the effect of the first laser pulse persists for some time and increases the photocurrent yield of the second pulse. The exponential slope of the measured signal corresponds to a time constant of about 30 fs. This time constant represents an upper time limit for the carrier injection process, since a vanishing correlation between the two laser pulses means also that the photo-carriers generated by the first laser pulse are gone when the second pulse arrives. The observation of a lifetime in the range of several tenths of femtoseconds rules out that a transient thermalized electron distribution is responsible for the effect, since the corresponding time constants would be in the range of picoseconds (see. e.g., [15]). Accordingly the measurement shown in Fig. 3a shows that a metal–insulator–metal junction under ultrashort pulse illumination can be utilized as an ultrafast electron injection device, extending the scheme of MIM based hot electron surface chemistry proposed by Gadzuk [16] to the time domain.

The observation of a lifetime, however, is also the crucial point to distinguish between photon-assisted tunneling and excited electron transport. Photon-assisted tunneling represents a direct coupling of an initial state on one side of the barrier with states on the other side of the barrier that are separated in energy by multiples of the photon energy. Therefore, no real intermediate states are involved that could give rise to lifetime effects. In contrast, transport of excited electrons involves intermediate states (Fig. 1) that can account for the observed lifetime. According to this, we conclude that the photocurrent signal in Fig. 3a is due to the transport of three-photon excited electrons. Since the transmission through the barrier drops rapidly below the tunnel barrier height this photocurrent is dominated by internal photoemission over the barrier.

In principle, the observed lifetime can be understood in a similar way as in time-resolved two-photon photoemission experiments, a technique that has been extensively used to investigate the electron dynamics at metal surfaces [17, 18]. In two-photon photoemission, the detected signal, i.e., the emitted electron, is the final state of a two-photon excitation process. Time resolved spectroscopy of the intermediate state that is exactly defined by the known final state energy, i.e., the kinetic electron energy and the photon energy, is achieved also in two-pulse correlation measurements. In case of time resolved photocurrent spectroscopy, the identification of the involved intermediate states is less obvious. In general, a large number of different pathways can contribute. However, a careful analysis of the spectral shape indicates that the excitation occurs via an interface state located on the Ag-oxide interface. Although a description of this analysis is beyond the scope of this paper and will be presented in a more extended paper [19], this demonstrates that time re-

solved photocurrent spectroscopy could become a valuable tool for the investigation of electrons dynamics at buried interfaces.

As discussed above the signal shown in Fig. 3a represents an almost pure three-photon process. However, such clear conditions are not always observed in the TPC measurements. Figure 3b shows the TPC spectrum measured in a different MIM junction for slightly lower laser intensity. In this spectrum, the signal enhancement for zero delay reaches only 22. Since alignment and phase stability are equivalent for both measurements, this lower enhancement must be attributed to a mixing of a second order and third order multiphoton processes. Higher order processes are ruled out, since they would lead to additional peaks in the Fourier spectrum, and as mentioned above, the linear process can be neglected due to its small quantum efficiency. The observed enhancement corresponds to a mixing ratio of two- and three-photon contributions of about 1:1. Accordingly, half of the photo-carriers are excited in a two-photon process and then have to tunnel through the barrier. The identification of this tunnel current contribution is interesting in the context of a recently proposed mechanism for an ultrafast scanning tunneling microscope [20]. Tunneling of two-photon excited electrons in a microscopic tunnel junction would provide a time-resolved signal with unprecedented spatial resolution.

The fact that two channels with different order of the multiphoton process can contribute to the same extent to the total transferred charge is closely related to the fact that a tunnel barrier suppresses the two-photon contribution with respect to the three-photon process. However, the excess energy of the injected carriers differs for both channels. This could be rather important for the femtochemistry of surface reactions that are based on a charge transfer between substrate and adsorbate, since the two competing channels deposit a different amount of energy per transferred charge.

The two-pulse correlation photocurrent measurements shown here reveal only two of the three transport mechanisms shown in Fig. 1, i.e., tunneling of excited electrons and internal photoemission. Consequently, one might assume that the applied laser intensity is just too low to give rise to photon-assisted tunneling or that the transport of excited electrons is always dominating. In a recent publication, we have presented experimental evidence that for similar laser intensities photon-assisted tunneling plays a role under rare experimental conditions [21]. The observation of photon-assisted tunneling depends critically on the interface properties that are difficult to control precisely in the preparation of the MIM junctions. The comparison with two theoretical models for photocurrents in MIM junctions indicates that photon-assisted tunneling is relevant when localized discrete interface states are involved in the transport [21].

In conclusion, the excitation of $Ag–Al_2O_3–Al$ junctions with ultrashort laser pulses induces a pulsed injection of electrons into the back electrode. Interferometric two-pulse correlation photocurrent measurements allow the identification of the dominant transport mechanisms: *i)* two-photon induced tunneling of excited electrons and *ii)* three-photon induced internal photoemission. In the present experiments, no current contribution due to photon-assisted tunneling has been identified. The experiment shown here demonstrates that two-pulse photocurrent correlation measurements allow to identify the photo-current transport mechanisms in intense fields. The time resolved signal also shows that the illumination of a MIM junction with ultrashort laser pulses leads to the injection of ultrashort electron pulses opening new possibilities for time-resolved spectroscopy of electron induced surface reactions.

ACKNOWLEDGEMENTS We thank H. Zacharias and A. Otto for stimulating discussions. This work has been supported by the Deutsche Forschungsgemeinschaft.

REFERENCES

1 A.H. Dayem, R.J. Martin: Phys. Rev. Lett. **8**, 246 (1962)
2 P.K. Tien, J.P. Gordon: Phys. Rev. **129**, 647 (1963)
3 M. Büttiker, R. Landauer: Phys. Rev. Lett. **49**, 1739 (1982)
4 F. Grossmann, T. Dittrich, P. Jung, P. Hänggi: Phys. Rev. Lett. **67**, 516 (1991)
5 C.A. Stafford, N.S. Wingreen: Phys. Rev. Lett. **76**, 1916 (1996)
6 J.T. York, R.D. Coalson, Y. Dahnovsky: Phys. Rev. B **65**, 235 321 (2002)
7 J. Lehmann, S. Kohler, P. Hänggi, A. Nitzan: Phys. Rev. Lett. **88**, 228 305 (2002)
8 M. Covington, M.W. Keller, R.L. Kautz, J.M. Martinis: Phys. Rev. Lett. **84**, 5192 (2000)
9 Z. Burshtein, J. Levinson: Phys. Rev. B **12**, 3453 (1975)
10 T. Brabec, F. Krausz: Rev. Mod. Phys. **72**, 545 (2000)
11 C. Lemell, X.M. Tong, F. Krausz, J. Burgdörfer: Phys. Rev. Lett. **90**, 076 403 (2003)
12 S.P. Apell, D.R. Penn: Phys. Rev. B **45**, 6757 (1992)
13 D. Diesing, A.W. Hassel, M.M. Lohrengel: Thin Solid Films **342**, 282 (1999)
14 B. Lamprecht, J.R. Krenn, A. Leitner, F.R. Aussenegg: Phys. Rev. Lett. **83**, 4421 (1999)
15 W.S. Fann, R. Storz, H.W.K. Tom, J. Bokor: Phys. Rev. Lett. **68**, 2834 (1992)
16 J.W. Gadzuk: Phys. Rev. Lett. **76**, 4234 (1996)
17 H. Petek, S. Ogawa: Prog. Surf. Sci. **56**, 239 (1997)
18 U. Höfer, I.L. Shumay, C. Reuss, U. Thomann, W. Wallauer, T. Fauster: Science **277**, 1480 (1997)
19 A. Thon, M. Merschdorf, D. Diesing, W. Pfeiffer: Phys. Rev. B *in preparation*
20 M. Merschdorf, W. Pfeiffer, A. Thon, G. Gerber: Appl. Phys. Lett. **81**, 286 (2002)
21 A. Thon, M. Merschdorf, W. Pfeiffer, T. Klamroth, P. Saalfrank, D. Diesing: Appl. Phys. A **78**, 189 (2004)